

Theory of strength and stability of kinetochore-microtubule attachments: collective effects of dynamic load-sharing

Dipanwita Ghanti,¹ Shubhadeep Patra,² and Debashish Chowdhury^{a1}

¹*Department of Physics, Indian Institute of Technology Kanpur, 208016, India*

²*ISERC, Visva-Bharati, Santiniketan 731235*

Measurement of the life time of attachments formed by a single microtubule (MT) with a single kinetochore (kt) *in-vitro* under force-clamp conditions revealed a catch-bond-like behavior. In the past the physical origin of this apparently counter-intuitive phenomenon was traced to the nature of the force-dependence of the (de-)polymerization kinetics of the microtubules. Here first the same model kt-MT attachment is subjected to external tension that is ramped up till the attachment gets ruptured; the trend of variation of the rupture force distribution with increasing loading rate is consistent with that displayed by the catch bonds formed in some other ligand-receptor systems. We then extend the formalism to model an attachment of a bundle of multiple parallel microtubules with a single kt under force-clamp and force-ramp conditions. From numerical studies of the model we predict the trends of variation of the mean life time and mean rupture force with the increasing number of MTs in the bundle. Both the mean life time and the mean rupture force display nontrivial nonlinear dependence on the maximum number of MTs that can attach simultaneously to the same kt.

^a Corresponding author; e-mail: debch@iitk.ac.in

I. INTRODUCTION

Multi-component molecular machines are assembled in a living cell at the right place at the right time. Assembling such a machine requires formation of molecular joints between specific components. However, molecular joints in these machines, unlike those in their macroscopic counterparts, are usually non-permanent. The *lifetime* and the *strength* are the two key characteristics of these molecular joints. How these properties of the joints depend on the (a) structure, and (b) dynamics of the participating components, and (c) interactions among these components are among the fundamental questions from the perspective of statistical thermodynamics and stochastic kinetics. Similar questions have been addressed by chemical physicists (or physical chemists) for many decades in the context of various types of ligand-receptor bonds. The main aim of this paper is to develop stochastic models for the kinetics of a class of molecular joints in a multi-component molecular machine and to compute its lifetime and strength to elucidate the consequences of the unusual structure, dynamics and interaction of the components that form this molecular joint. More specifically, the molecular joint that we investigate in this paper is formed in a multi-component macromolecular machine called mitotic spindle [1–3]. This self-organized machine carries out mitosis [4], the process of segregation of replicated chromosomes, in eukaryotic cells.

One of the major components of a spindle is a stiff filament called microtubule (MT) [5] each of which has a tubular structure. The unique feature of the kinetics of a MT is dynamic instability [6]. A polymerizing MT keeps growing in length till it suffers “catastrophe” whereby it abruptly begins to depolymerize. A depolymerizing MT would, eventually, disappear unless its rapid shrinkage is stopped by a process called ‘rescue’ following which it resumes polymerization. Because of the sequence of catastrophe and rescue, a single MT can exhibit several alternate phases of polymerization and depolymerization. On the surface of each sister chromatid, that results from DNA replication, a proteinous complex called kinetochore (kt) is located [7]. During the self-assembling of the spindle each kt attaches with one or more MTs; the actual number varies from one species to another. The kt-MT attachment in budding yeast is known to be the simplest; each kt can attach with only a single MT [8]. Significant progress has been made in the last few years in understanding this simple kt-MT attachment after successful reconstitution of its kinetochore *in-vitro* [8, 9]. However, the identity of all the molecular components of the coupler and its structure as well as its energetic stability and kinetics are currently under intense investigation [9–11]. Complementary work on biochemical reconstitution of mammalian kinetochores has just begun [12].

The kt-MT attachments have many similarities with the chemical ligand-receptor bonds; the kt is the analog of the receptor while each MT is the counterpart of a ligand. However, in spite of these superficial similarities, there are several crucial differences. For example, the tip of each MT remains free to polymerize/depolymerize and rapid turnover of its monomeric subunits continues even when the attachments remains intact. Moreover, force plays all the three roles, namely, input, output and signal, for different components of the same kt-MT attachment. As the key force generators in mitosis, the MTs play crucial roles in proper positioning of the chromosomes. Equally important is the opposing force exerted by the depolymerizing MTs attached to the two sister chromatids that eventually pull the two sister chromatids apart and away from each other in the late stages of mitosis [4]. It is the molecular joint formed by the attachment of N parallel MTs to a single kt (where $N \geq 1$), that we study here from the perspective of chemical physics/ physical chemistry by treating it an unusual ligand-receptor bond.

One of the counter-intuitive results has been obtained in the recent past from *in-vitro* experiments where an external tension was applied on a single kt-MT attachment with an optical trap [13]. The stability was found to increase with increasing force provided the force was not too large; beyond a moderate level further increase of the force, of course, reduced the stability of the attachment. More specifically, in these “force-clamp” experiments the magnitude of the pulling force was kept fixed and the lifetime of the attachment (i.e., the time taken to get ruptured) was measured. The non-monotonic variation of the average lifetime with increasing strength of the pulling force is reminiscent of catch-bonds formed by wide varieties of ligands with their respective receptors [14–17].

In an earlier paper one of the authors (DC) of this paper (with two other co-authors) [18] developed a minimal theoretical model (from now onwards referred to as SSC model) to account for the observed catch-bond like behavior of the kt-MT attachment in budding yeast. This work elucidated the crucial role of MT kinetics (particularly its force-dependence) that makes this catch-bond fundamentally different from the common catch-bonds in chemical ligand-receptor systems in spite of their superficial similarities. It also indicated the conditions under which the same system would exhibit a slip-bond-like, instead of catch-bond like, behavior. However, the theory was developed in ref.[18] only for the force-clamp situation, i.e., for the calculation of lifetime distribution when the applied tension was held constant.

In this paper we first adapt the SSC model to calculate the distribution of the rupture force under force-ramp conditions where the pulling force is increased with the passage of time. We draw attention to the similar trends of variation of the rupture force distribution reported earlier for catch-bonds formed in other ligand-receptor systems. We then extend the model to mimic the kt-MT attachments in mammalian cells where up to a maximum of N (> 1) parallel MTs can simultaneously attach to a single kt. In principle, our theoretical predictions for $N = 1$ can be

tested using the reconstituted kinetochore of budding yeast *in-vitro* applying standard techniques of dynamic force spectroscopy [19]; a typical set up would use an optical trap with controlled ramp protocol [10]. Recent reconstitution of mammalian kt *in-vitro* [12] indicates promising new routes for testing our results for $N > 1$.

II. SSC MODEL: FROM FORCE-CLAMP TO FORCE-RAMP FOR $N = 1$

In this section we present a brief summary of the adaptation of the continuum formulation of the SSC model, as well as its discretization, that is appropriate for theoretical analysis of the force-ramp scenario. The SSC model [18] is a minimal model in the sense that it does not make any assumption about the molecular constituents or structure of the kt-MT attachment; it merely assumes a cylindrical “sleeve-like” coupler (in the spirit of the Hill sleeve model [20]) that is coaxial with the MT and has a diameter slightly larger than that of the MT. The sleeve may be an abstract representation of the Dam1 ring [21] while the “rigid rod”, that connects the sleeve with the kinetochore, captures the effects of Ndc80 proteins [22–24].

In this model the instantaneous overlap between the outer surface of the MT and the inner surface of the coaxial cylindrical sleeve is represented by a continuous variable $y(t)$ which is a function of time t . The total length of the coupler is L so that $0 \leq y(t) \leq L$. Two main postulates of this model are as follows [18]:

Postulate (a): increasing overlap y lowers the energy of the system and that this lowering of energy is proportional to y so that the kt-MT interaction potential $V_b(y)$ is assumed to have the form

$$V_b(y) = -By, \quad (1)$$

where B is the constant of proportionality. Accordingly, the magnitude of the depth of the potential at $y = L$ is BL . Postulate (b): the external force F suppresses the rate of depolymerization β of the MT and that β decreases exponentially with increasing F following

$$\beta(F) = \beta_0 \exp(-F/F_\star), \quad (2)$$

where β_0 is depolymerization rate in the absence of any external force and the parameter F_\star is a characteristic force that determines the sharpness of the decrease of $\beta(F)$ with F .

The postulate (a) is essentially a limiting case of the Hill model in the sense that the “roughness” of the interface between the outer surface of the MT and inner surface of the sleeve is neglected in the minimal version of the SSC model. The postulate (b) is qualitatively supported by the *in-vitro* experiments of Franck et al. [25]. The decrease of the rate β with the external force F need not be exponential; all the conclusions drawn from the SSC model in ref.[18] remain valid as long as the decrease of β with increasing F is sufficiently sharp.

The kinetics of this model kt-MT attachment can be formulated in terms of a Fokker-Planck (FP) equation [26] for the probability density $P(y, t)$. The attachment survives as long as y remains non-zero; the rupture of the attachment is identified with the attainment of the value $y = 0$ *for the first time*. For the calculation of the lifetime of the attachment a unique initial condition is required. In ref.[18] the authors assumed that initially (i.e., at time $t = 0$) the MT is fully inserted into the sleeve, i.e.,

$$y(t = 0) = L \quad (\text{initial condition}). \quad (3)$$

Since the MT is not allowed to penetrate the kinetochore plate, the overlap y cannot exceed L . This physical condition is captured mathematically by imposing the *reflecting* boundary condition

$$J(y, t)|_{y=L} = 0. \quad (4)$$

An absorbing boundary condition

$$P(y, t)|_{y=0} = 0 \quad (5)$$

is imposed at $y = 0$ for the calculation of the life times. Starting from the initial condition (3), the time taken by the system to attain vanishing overlap ($y = 0$) *for the first time* was identified as the life time of the attachment. This lifetime fluctuates from one kt-MT attachment to another; the distribution of the lifetime contains all the statistical information.

The FP equation for $y(t)$ can be viewed as that for the position of a hypothetical Brownian particle, subjected to an external potential $V(y) = -By + Fy$, in a one dimensional space with a reflecting boundary at $y = L$ and an absorbing boundary at $y = 0$. The calculation of the lifetime is essentially that of a *first passage time* for the Brownian particle: the time it takes to reach $y = 0$ for the first time starting from $y = L$ at $t = 0$. In ref.[18] the authors

calculated the exact distribution of the lifetimes analytically in the Laplace space and hence the mean lifetime $\langle t \rangle$ to be

$$\langle t \rangle = \frac{D}{v^2(F)} \left[e^{v(F)L/D} - 1 \right] - \frac{L}{v(F)} \quad (6)$$

where D is the diffusion constant of the hypothetical Brownian particle while its net drift velocity $v(F)$ is given by

$$v(F) = \frac{B - F}{\Gamma} + (\alpha - \beta(F))\ell \quad (7)$$

where ℓ is the length increased by the addition of each subunit of the MT and Γ is the phenomenological coefficient that characterizes the viscous drag.

For the convenience of numerical computation of the distribution of the lifetimes by computer simulation, the SSC model was discretized in ref.[18] following prescriptions proposed earlier by Wang, Peskin and Elston (WPE) [27, 28]. Following WPE, space was discretized into M cells, each of length $h = L/M$ and the continuous effective potential $\tilde{U}(x)$ was replaced by its discrete counterpart

$$\frac{\tilde{U}_j}{k_B T} = \left[\frac{(F - B)}{k_B T} + \ell \frac{\left(\beta_{max} e^{-F/F_*} - \alpha \right)}{D} \right] x_j \quad (8)$$

where x_j denotes the position of the center of the j -th cell. In the discrete formulation, instead of a FP equation, a master equation describes the kinetics of the system in terms of discrete jumps of the hypothetical Brownian particle from the center of a cell to that of its adjacent cells, either in the forward or in the backward direction. The rates of forward and backward jumps $\omega_f(j)$ and $\omega_b(j)$ on the discretized lattice were given by [27]

$$\omega_f(j) = \frac{D}{h^2} \frac{-\frac{\delta \tilde{U}_j}{k_B T}}{\exp\left(-\frac{\delta \tilde{U}_j}{k_B T}\right) - 1} = \frac{1}{h} \frac{\frac{B - F}{\Gamma} + \ell(\alpha - \beta)}{\exp\left(-\frac{\delta \tilde{U}_j}{k_B T}\right) - 1} \quad (9)$$

$$\omega_b(j) = \frac{D}{h^2} \frac{\frac{\delta \tilde{U}_j}{k_B T}}{\exp\left(\frac{\delta \tilde{U}_j}{k_B T}\right) - 1} = \frac{1}{h} \frac{\frac{F - B}{\Gamma} + \ell(\beta - \alpha)}{\exp\left(\frac{\delta \tilde{U}_j}{k_B T}\right) - 1} \quad (10)$$

where

$$\delta \tilde{U}_j = \tilde{U}_{j+1} - \tilde{U}_j \quad (11)$$

Excellent agreement between the results derived from the analytical theory and computer simulations was reported in ref.[18].

The external pulling force F has two opposite effects on the MT. On the one hand, the MT is bodily pulled out of the coupler by F . On the other hand, because of the suppression of the depolymerization rate β by the external pull F , the polymerization can dominate over depolymerization resulting in a net growth of the MT. If the increase in y resulting from the net growth of the MT can more than compensate the decrease in y caused by the bodily movement of the MT out of the coupler, the net result will be an increase of y . Such an increase of y , instead of the naively expected decrease, upon application of F would be interpreted as an effective increase of the stability of the kt-MT attachment with increasing strength of the applied force F . However, as the strength of F increases, $\beta(F)$ gradually saturates. Since β practically stops decreasing further with the further increase of F the bodily movement of the MT out of the coupler at higher values of F can no longer be compensated by the tip growth into the coupler; the net decrease of y with further increase of F in this regime manifests as decrease in the stability of the kt-MT attachment. Such overall non-monotonic variation of the mean life time $\langle t \rangle$ with F is interpreted as a catch bond-like behavior of the kt-MT attachment. However, increase of $\langle t \rangle$ with F in the small F regime is possible only if $\beta(F)$ decreases sufficiently sharply with increasing F . Otherwise, the kt-MT attachment would behave effectively as a slip bond.

In ref.[18] the external F was assumed to be independent of time t ; these corresponds to a “force-clamp” situation in the experiments. In this section the time-dependent external force $F(t)$ is assumed to increase according to a well defined protocol; this corresponds to a “force-ramp” in experiments. We adopt the postulates (a) and (b) of the SSC model. For the sake of simplicity, we assume a linear ramp force, namely, $F(t) = at$ where a is loading

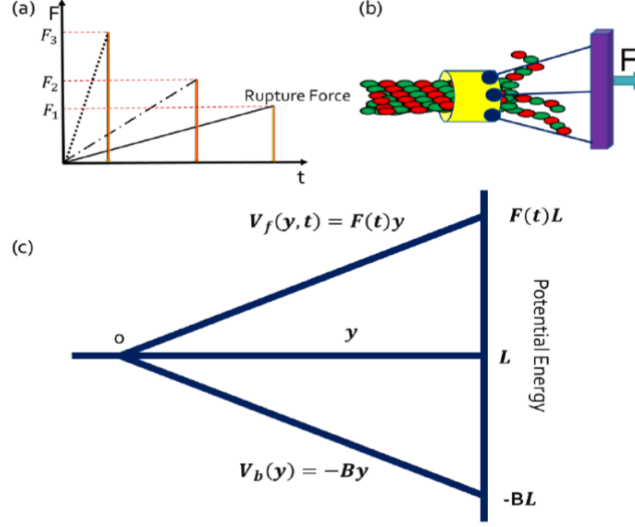


FIG. 1. (a) Linearly increasing force ($F = at$); different straight lines correspond to different rates of loading. The kt-MT attachment survives the increasing tension up to a certain time and then gets ruptured. (b) A schematic depiction of the kt-MT attachment in the presence of external force. (c) Hypothesized effective potentials $V_b(y)$ and $V_f(y, t)$ are plotted against the instantaneous length of overlap $y(t)$.

rate. The instantaneous external force $F(t)$ can be derived from the corresponding instantaneous potential landscape, $V_f(y, t) = F(t)y$. The effective potentials $V_b(y)$ and $V_f(y, t)$ at an arbitrary instant of time are plotted in Fig.1. Net instantaneous potential $V(y, t)$ felt by the kinetochore is $V(y, t) = V_b(y) + V_f(y, t)$.

For the theoretical treatment of the kt-MT attachment subjected to a ramp force $F(t)$, we adapt the corresponding theory for ligand-receptor bond rupture, developed originally by Bell [29] and subsequently extended by Evans and Ritchie [30] and by Evans and Williams [32] (see also the reviews in refs.[34, 35]). In the presence of a given force F , let $k_{on}(F)$ and $k_{off}(F)$ be the rates of binding and unbinding, respectively, of a MT to the kt mediated by the coupler. Because of the specific choice of the initial condition $y(t=0) = L$ and the absorbing boundary condition at $y = 0$, no rebinding of the MT is possible and, therefore, we can put $k_{on}(F) = 0$. Denoting the probability that $y \neq 0$ (i.e., MT is attached to the kt) at time t by the symbol $P_{on}(t)$, the equation governing the time evolution of $P_{on}(t)$ is

$$\frac{dP_{on}(t)}{dt} = -k_{off}(F)P_{on}(t). \quad (12)$$

Hence, in terms of $k_{off}(F)$, the survival probability $S(t)$ of the attachment (i.e., the probability that the hypothetical Brownian particle has not reached $y = 0$ before time t) can be expressed as [34]

$$S(t) = \exp\left[-\int_0^t k_{off}(F(t'))dt'\right] \quad (13)$$

Moreover, in terms of $k_{off}(F)$ the probability density $\rho_{fp}(F)$ of the rupture forces is expressed as [34]

$$\rho_{fp}(F) = \frac{k_{off}(F)}{a} \left[\exp\left(-\frac{1}{a} \int_0^F k_{off}(F')dF'\right) \right] \quad (14)$$

Thus, for the calculation of $S(t)$ and $\rho_{fp}(F)$ the analytical expression for $k_{off}(F)$ is required. For $k_{off}(F)$ we use the expression for the inverse of the average lifetime of a single kt-MT attachment in the SSC model, reported in ref.[18], namely,

$$k_{off}(F) = \frac{1}{\langle t \rangle} = \frac{v^2(F)}{D(e^{v(F)L/D} - 1) - Lv(F)} \quad (15)$$

where the expression $v(F)$ is given by Eq.(7). Substituting Eq.(15) into the Eqs.(13) and (14) we get, respectively, the survival probability $S(t)$ and the rupture force density $\rho_{fp}(F)$ by numerically evaluating the respective integrals.

Parameter	Values
Inter-space between MT binding site l [20, 36, 37]	$8/13 \text{ nm}$
Total length of coupler L [38–41]	50 nm
Polymerization rate α [20, 36, 37, 42]	30 s^{-1}
Maximum Depolymerization rate β_0 [20, 36, 37, 42]	350 s^{-1}
Characteristic force of Depolymerization F_* [18]	0.8 pN
Attractive force between kt-MT B [18]	1.9 pN
Diffusion constant D [20, 36, 37]	$700 \text{ nm}^2 \text{ s}^{-1}$
Viscous drag coefficient Γ [20, 36, 37, 43]	$6 \text{ pNs } \mu^{-1}$

TABLE I. Values of the parameters for kt-MT system

For computer simulation of the model, we discretize the continuum version of the SSC model following WPE prescription [27, 28] as explained in ref.[18]. Instead of a constant force, a time-dependent external force $F = at$ is imposed. Carrying out computer simulations of this discretized version of the model we directly compute the survival probability $S(t)$ and the distribution $\rho_{fp}(F)$ of the rupture forces. Throughout this section lines and discrete points, respectively, have been used to plot the theoretical results derived from numerical integrations of eqns.(13)- (14) and the data obtained from computer simulations of the discretized model. Parameter values that we used for numerical calculations are listed in table I.

A. Result for the rupture of kt-MT attachment under ramp force for $N=1$

In the Fig.2(a) the rupture force distribution obtained from numerical integration of the eqns.(13)-(14) of the continuum theory and those obtained from computer simulation of the discretized model are plotted for four different loading rates. At loading rates as low as $a = 3 \times 10^{-4} \text{ pNs}^{-1}$ (violet), the most probable rupture force is vanishingly small. At such slow loading rates the rupture of the attachment is mostly spontaneous dissociation caused by thermal fluctuation and is very rarely driven by the applied tension. However, as the loading rate increases a second peak at a non-zero value of the force begins to emerge. At moderate loading rates like $a = 1 \times 10^{-3} \text{ pNs}^{-1}$ (blue line and triangle) and $a = 3 \times 10^{-3} \text{ pNs}^{-1}$ (green line and square)), a large fraction of the kt-MT attachments survive upto a high force before getting ruptured while another significant fraction of the attachments still dissociate at a vanishingly small force. But, at sufficiently high rates of loading, for example at $a = 3 \times 10^{-2} \text{ pNs}^{-1}$ (red), an overwhelmingly large fraction survives up to a high force while very few attachment get ruptured by very weak forces. The existence of two peaks at intermediate rates of loading, where the peak at non-zero force rises with increasing loading rate while that at the vanishing force decreases, is a key signature of catch bonds established by force-ramp experiments with other well known catch bonds [45].

In the Fig.2(b) the survival probabilities are plotted at the same loading rates for which the rupture force distributions have been plotted in Fig.2(a). For the same set of parameter values, the data in the Figs.2(a) and (b) are consistent with each other. At very high loading rates the probability of survival remains high, and practically unaffected by the applied force, upto quite high values of the force and, accordingly, the most probable rupture force is also expected to be high. In contrast, sharp drop in the survival probability with increasing force is also reflected in the vanishingly small most probable rupture force at very low loading rates. In the Fig.2(c) we have plotted mean rupture force as a function of loading rate. Mean rupture force increases with increasing loading rate.

The increase of mean and most probable rupture force with increasing loading rate is also observed in case of common ligand-receptor attachments [34]; it follows from the mathematical form of the equation

$$\frac{dP_{on}(F)}{dF} = -\frac{1}{a}k_{off}(F)P_{on}(F) \quad (16)$$

which is nothing but the equation (12) expressed in terms of force F rather than time t . Eqn.(16) implies that the rate of decay of the bound state of the bond is inversely proportional to the loading rate a . Consequently, the ligand-receptor bond persists up to higher values of force when subjected to faster loading rates.

B. Comparison between Dogterom-Leibler model and SSC model

It is worth pointing out that the FP equation describing the stochastic evolution of the probability density of the overlap variable x in the SSC model does not have any explicit terms describing catastrophe and rescue [6]. In order to justify their absence and to explain the nature of the approximations let us begin with the Dogterom-Leibler model

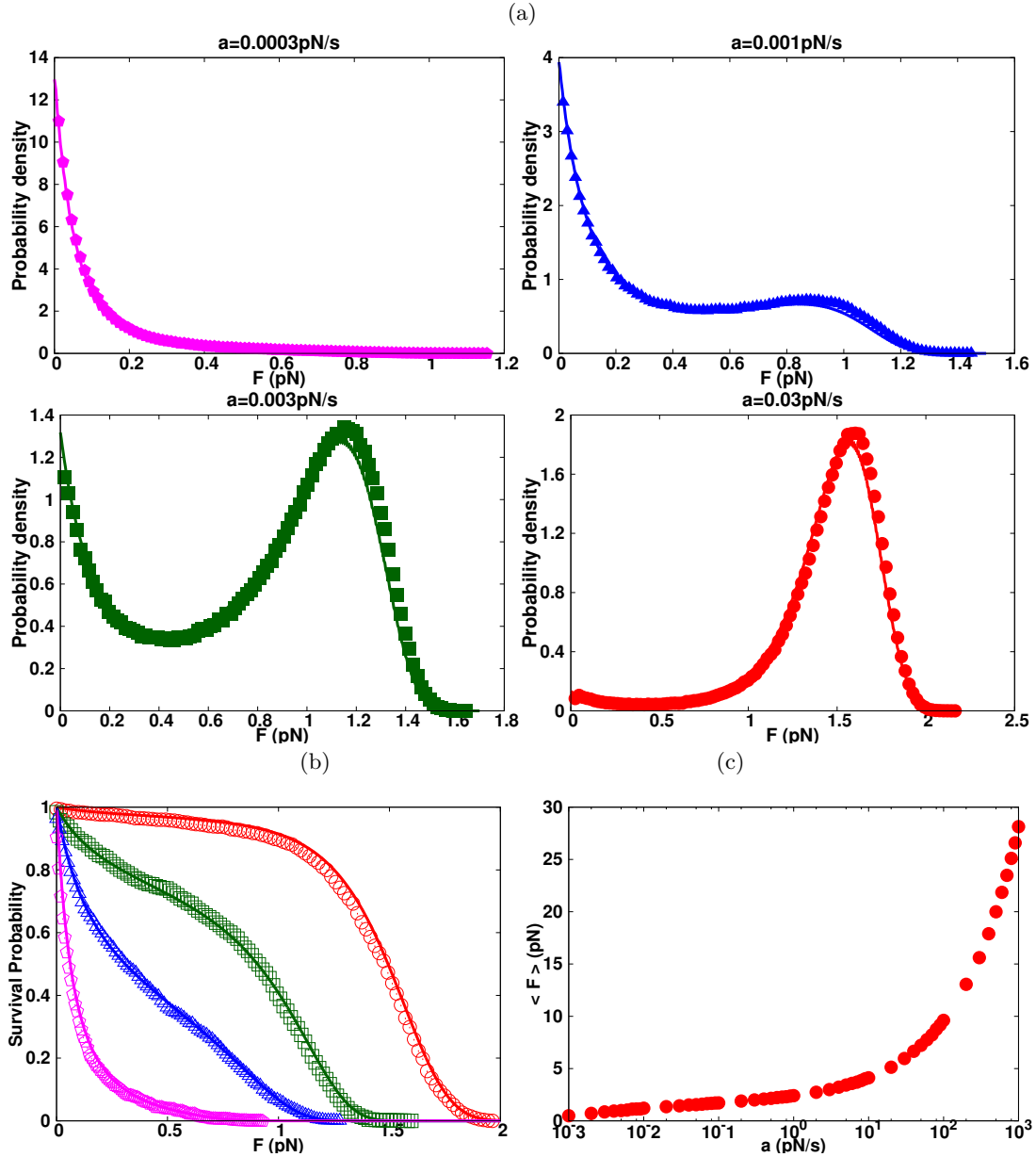


FIG. 2. (a) Probability density of rupture force of the kt-MT attachment with $N = 1$ for four different loading rates, namely, $a = 3 \times 10^{-4} \text{pNs}^{-1}$ (violet pentagon), $a = 1 \times 10^{-3} \text{pNs}^{-1}$ (green square), $a = 3 \times 10^{-3} \text{pNs}^{-1}$ (blue triangle) and $a = 3 \times 10^{-2} \text{pNs}^{-1}$ (red circle) are plotted. The continuous curves have been plotted by numerical integration of the Eq.(14) whereas the discrete data points have been obtained from computer simulations of the discretized version of the same model. (b) Survival probability for different loading rates; the same symbols in (a) and (b) correspond to the same set of values of the model parameters. (c) Mean rupture force is plotted against the logarithm of the loading rate. Numerical values of all the other parameters are listed in table-I.

[46] that describe the polymerization-depolymerization of MTs in terms of mathematical equations. Let v_p and v_d denote the average speeds of polymerization and depolymerization, respectively, while c and r are the corresponding rates of catastrophe and rescue of the MTs. In that model the stochastic equations governing the time evolution of the probability densities P_{\pm} of the polymerizing (+) and depolymerizing (-) MTs are given by

$$\begin{aligned} \frac{\partial P_+(x, t)}{\partial t} + v_p \frac{\partial P_+(x, t)}{\partial x} &= -cP_+(x, t) + rP_-(x, t) \\ \frac{\partial P_-(x, t)}{\partial t} - v_d \frac{\partial P_-(x, t)}{\partial x} &= -rP_-(x, t) + cP_+(x, t) \end{aligned} \quad (17)$$

In the context of the kt-MT coupler, let us re-interpret the symbols $P_{\pm}(x, t)$ as the probability densities of overlap x of polymerizing (+) and depolymerizing (-) MTs with the coaxial cylindrical coupler at time t . In principle, the eq.(17) would still describe the time evolution of $P_{\pm}(x, t)$ where the rate constants would be force-dependent. Now adding both the Eqn.(17), and defining the total probability density $P(x, t) = P_+(x, t) + P_-(x, t)$ we get the FP eq.

$$\frac{\partial P(x, t)}{\partial t} + (v_p - v_d) \frac{\partial P(x, t)}{\partial x} = 0 \quad (18)$$

only if $\frac{\partial P_+(x, t)}{\partial x} = \frac{\partial P_-(x, t)}{\partial x}$. Incorporating the extra terms arising from the diffusion of the kinetochore plate, the effective force B arising from the MT-coupler interaction and the external tension F in eq.(18) we get the FP eqn. of the SSC model (eqs. (6) and (7) of ref.[18]) identifying v_p and v_d with α and β , respectively. This comparison with the Dogterom-Leibler equations not only shows how the terms corresponding to catastrophe and rescue in the equation for P_+ cancel out those in the equation for P_- but also establishes the nature of the approximation made in writing the FP eqn for the SSC model in ref.[18].

C. Comparison between Dogterom-Leibler model and Akiyoshi et al.'s model

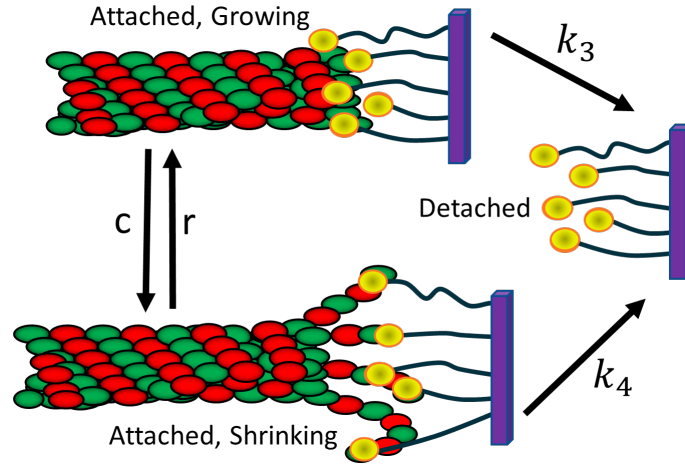


FIG. 3. MT is attached with Kt and switching between growing and shrinking phase with frequency c and r . It can detach from Kt with rate k_3 and k_4 .

Akiyoshi et al. [13] used a simple kinetic model to account for their experimental data. In that model each MT can switch between the states of polymerization and depolymerization with the catastrophe and rescue frequencies c and r , respectively. While still attached to the kt, a MT can detach with the rate k_3 or k_4 depending on whether it is in the state of polymerization or depolymerization at that instant of time (see Fig.3). We extend the Dogterom-Leibler equations incorporating the detachment process; the resulting equations are

$$\begin{aligned} \frac{\partial P_+(x, t)}{\partial t} + v_p \frac{\partial P_+(x, t)}{\partial x} &= -(c + k_3)P_+(x, t) + rP_-(x, t) \\ \frac{\partial P_-(x, t)}{\partial t} - v_d \frac{\partial P_-(x, t)}{\partial x} &= -(r + k_4)P_-(x, t) + cP_+(x, t) \end{aligned} \quad (19)$$

Defining $\int P_{\pm}(x, t)dx = P_{\pm}(t)$ and integrating both sides of the eq.(19) with respect to x , we get

$$\begin{aligned} \frac{\partial P_+(t)}{\partial t} + v_p P_+(t) &= -(c + k_3)P_+(t) + rP_-(t) \\ \frac{\partial P_-(t)}{\partial t} - v_d P_-(t) &= -(r + k_4)P_-(t) + cP_+(t) \end{aligned} \quad (20)$$

The stochastic equations used by Akiyoshi et al.[13]

$$\begin{aligned} \frac{\partial P_+(t)}{\partial t} &= -(c + k_3)P_+(t) + rP_-(t) \\ \frac{\partial P_-(t)}{\partial t} &= -(r + k_4)P_-(t) + cP_+(t) \end{aligned} \quad (21)$$

follows only if the terms with v_p and v_d are neglected. In other words, compared to Dogterom-Leibler scenario, the terms corresponding to polymerization and depolymerization are absent from the kinetic equations used by Akiyoshi model in analyzing their data. Thus, the SSC model [18] and the kinetic model presented by Akiyoshi et al.[13] are complementary to each other in the sense that the catastrophe and rescue terms are absent in the former whereas the polymerization and depolymerization terms are absent in the latter.

III. EXTENDED SSC MODEL OF MT- SINGLE KT ATTACHMENT FOR $N > 1$

In this section we extend the SSC model to capture some key features of the energetics and kinetics of a dynamic attachment formed between a single kt and a bundle of N parallel MTs. We study the strength and stability of this model attachment by computer simulation of dynamic force spectroscopy under both force-clamp and force-ramp conditions.

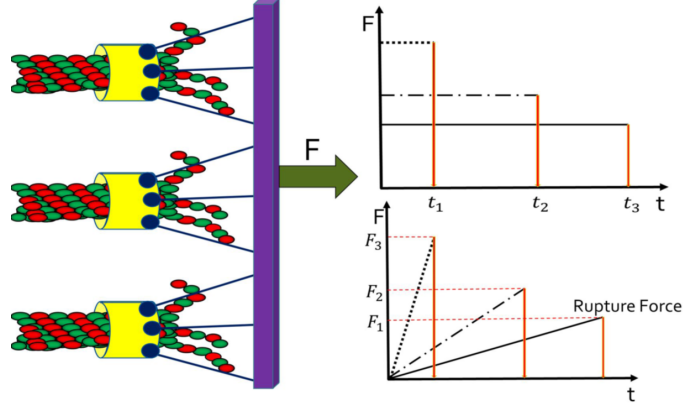


FIG. 4. Three microtubule single kinetochore attachment in the presence of external force on kinetochore (violet wall). Two types of external force are applied, constant over time (force clamp) and linearly increasing with time (force ramp).

In this extended SSC model at any arbitrary instant of time t , a single kt is attached to $n(t)$ ($1 \leq n(t) \leq N$) parallel MTs, each through its respective coupler, where N is the maximum number of MTs that can attach to the kt simultaneously. For simplicity, all the couplers are assumed to have identical length L . The MTs are not directly coupled by any lateral bond (transverse to their axis). Instead, all the collective effects arise from their indirect coupling via the kinetochore to which $n(t)$ MTs are attached. The physically motivated assumption of the model, which couple their kinetics is that at any instant of time t , the externally applied load tension F is shared equally among the $n(t)$ MTs that are attached to the kt at that instant through their respective couplers, i.e., $F/n(t)$. This assumption indicates that the forced detachment of one MT from the kt can increase the likelihood of that of the surviving ones through re-distribution of the load force F . We consider two possible scenarios for the rupture of a joint formed by a kt initially with multiple MTs. In the first, once a MT detaches, its re-attachment to the same kt is not allowed. Number of MT N attached with kt varies irreversibly as

$$N \rightarrow N - 1 \rightarrow N - 2 \rightarrow N - 3 \rightarrow \dots \rightarrow 2 \rightarrow 1 \rightarrow 0 \quad (22)$$

In the second scenario, once a MT detaches it can reattach again to the same kt and can grow inside the coupler because of its polymerization. So, in this case, the number of MT N attached to the kt varies reversibly as

$$N \rightleftharpoons N - 1 \rightleftharpoons N - 2 \rightleftharpoons N - 3 \rightleftharpoons \dots \rightleftharpoons 2 \rightleftharpoons 1 \rightarrow 0 \quad (23)$$

IV. SIMULATION METHOD

Extending the WPE prescription [27, 28] used earlier for the single MT-kt attachment, space is now discretized into M cells, each of length $h = L/M$. Then the time-dependent discrete effective potential is given by

$$\frac{U_{nj}}{k_B T} = \left[\frac{\left(\frac{F}{n(t)} - B \right)}{k_B T} + \ell \frac{\beta_{max} e^{-\frac{F/n(t)}{F_*}} - \alpha}{D} \right] x_j \quad (24)$$

where $n(t)$ is the number of MTs attached to the kt at the instant of time t . Accordingly, the corresponding forward ($w_{fn}(j)$) and backward ($w_{bn}(j)$) transition rates are given by [27]

$$w_{fn}(j) = \frac{D}{h^2} \frac{-\frac{\delta U_j}{k_B T}}{\exp(-\frac{\delta U_j}{k_B T}) - 1} \quad (25)$$

$$w_{bn}(j) = \frac{D}{h^2} \frac{\frac{\delta U_j}{k_B T}}{\exp(\frac{\delta U_j}{k_B T}) - 1} \quad (26)$$

Where $\delta U_{nj} = U_{nj+1} - U_{nj}$. In our simulation of both the scenarios mentioned above, initially, all the N MT are fully inserted into the kt coupler.

In the first scenario, using the transition rates given by eq.(25) and eq.(26) the position of a MT tip inside its coupler is updated. But, once an attachment breaks its reattachment to the kt is not allowed; therefore, detached MT is no longer monitored in our simulation. However, the simulation is continued till the last surviving MT-kt attachment just breaks down. This first passage time is identified as the life time of the molecular joint consisting of N MT with a single kt. The process is repeated many times, starting from the same initial condition, to obtain the distribution of the lifetimes. In the same scenario, under the force-ramp condition ($F = at$) we collect the data similarly to obtain the distribution of rupture forces (i.e., the force at which the tip of the last surviving MT tip exits from its coupler).

In the alternative scenario, the transition rates eq.25 and eq.26 govern the kinetics of the tip of each MT as long as it moves inside the corresponding coupler. However, once the attachment between a MT and the kt, through the coupler, breaks down it must get an opportunity to reattach through its natural kinetics of polymerization and depolymerization outside the coupler. Therefore, in this scenario, the continuing forward and backward movement of the tip of a detached MT outside its coupler is monitored in our simulation. During this period the force-free kinetics of the MT tip outside its coupler is implemented in our simulation by replacing the potential (24) by the simpler potential

$$\frac{V_j}{k_B T} = \ell \left[\frac{\beta_{max} - \alpha}{D} \right] x_j \quad (27)$$

and simultaneously replacing the transition rates (25) and (26) by

$$w_{f1}(j) = \frac{D}{h^2} \frac{-\frac{\delta V_j}{k_B T}}{\exp(-\frac{\delta V_j}{k_B T}) - 1} \quad (28)$$

and

$$w_{b1}(j) = \frac{D}{h^2} \frac{\frac{\delta V_j}{k_B T}}{\exp(\frac{\delta V_j}{k_B T}) - 1}, \quad (29)$$

respectively, where $\delta V_j = V_{j+1} - V_j$. If, through this kinetics outside the coupler, a MT succeeds in re-entering its coupler its kinetics reverts back to that governed by the transition rates eq.25 and eq.26. Thus, starting from the initial state the time evolution of all the MTs are monitored till the instant when, for the first time, none of the MTs is attached to the kt; this first-passage time is identified as the lifetime of the attachment. Repeating this process we have obtained the distributions of the lifetimes in the second scenario. Similarly for the ramp force we have obtained the distribution of the rupture force which is defined as the force at which, for the first time, none of the MTs is attached to the kt.

A. Results on life time distribution under clamp force for $N > 1$

In Fig.5 (a) and (b) survival probabilities of an attachment, consisting initially of 40 MTs and a single kt, have been plotted as a function of time for the two cases where rebinding is (a) forbidden and (b) allowed, respectively. The attachment survives for longer duration in intermediate range of the clamp force ($F = 0.5\text{pN}$, blue square) than at the high and low strength of the tension. In the inset the corresponding distributions of the lifetimes of the attachments are also shown.

The trends of variation of the survival probability with the clamp force indicates a catch-bond-like behavior. Indeed, this catch-bond-like behavior can be seen directly in Fig.5(c) where the mean life time $\langle t \rangle$, plotted against the clamp force F , displays a maximum at a non-zero finite value of F irrespective of whether rebinding of the MTs is allowed or forbidden. The physical cause of the catch-bond-like behavior is the same as that pointed out in the special case $N = 1$. Moreover, as expected on physical grounds, for any given F , the mean life time $\langle t \rangle$ is higher if rebinding is allowed as compared to the mean life time in the absence of rebinding.

In the Fig.5(d) mean lifetime is found to increase with the number of microtubule (N). This is consistent with one's intuitive expectation. Besides, for any given value of N , allowing rebinding of the MTs results in a higher life time. However, the interesting point is that the mean life time increases nonlinearly with N in both the cases.

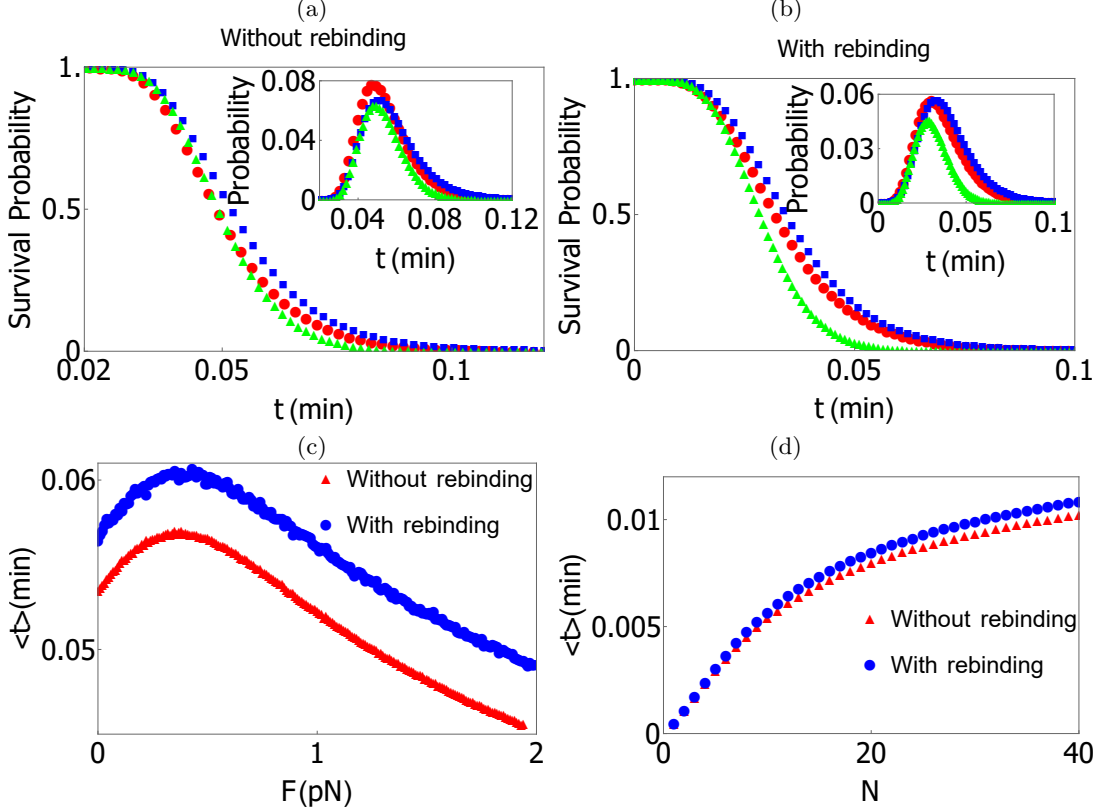


FIG. 5. Survival probability is plotted as a function of time t , under force clamp condition (a) in the absence of rebinding, for three different values of the tension, $F = 0.01$ pN, (red circle), $F = 0.5$ pN (blue square) and $F = 1$ pN (green triangle), and (b) in the presence of rebinding, for three values of the tension $F = 0.01$ pN (red circle), $F = 0.6$ pN (blue square) and $F = 1.5$ pN (green triangle). In the insets of both the figures the corresponding distributions of the lifetimes are shown. The mean life time $\langle t \rangle$ is plotted against (c) tension F for $N = 40$ and (d) number N for $F = 10$ pN, $B = 0.5$ pN, each for both the scenarios, namely with rebinding (blue circle) and without rebinding (red triangle). The numerical values of all the other parameters used in the simulation are listed in the table I.

B. Results on rupture force distribution under force ramp for $N > 1$

In the Fig.6(a) and (b) survival probabilities (and the corresponding rupture force distribution in the insets) are plotted, respectively, in the absence and presence of rebinding for three different loading rates $a = 18$ pN/s, 20 pN/s and 22 pN/s. Survival probability remains high upto a certain force beyond which it drops quite sharply. In the Fig.6(c) and (d) the average rupture force is plotted, respectively, against the loading rate a (for a given N) and against N (for a given loading rate a). The log-scale along the X-axis in Fig.6(c) is used to cover a wide range of loading rates in the most suitable manner. The higher survival probability caused by reattachment of MTs is more pronounced at slower loading than at faster loading. This trend of variation follows from the fact that at faster loading detached MTs get smaller chances of reattaching before the complete rupture of the attachment. What is interesting from the quantitative point of view is that the average rupture force increases nonlinearly with increasing loading rate. Finally,

the increase of the mean rupture force with increasing N also seems to be nonlinear.

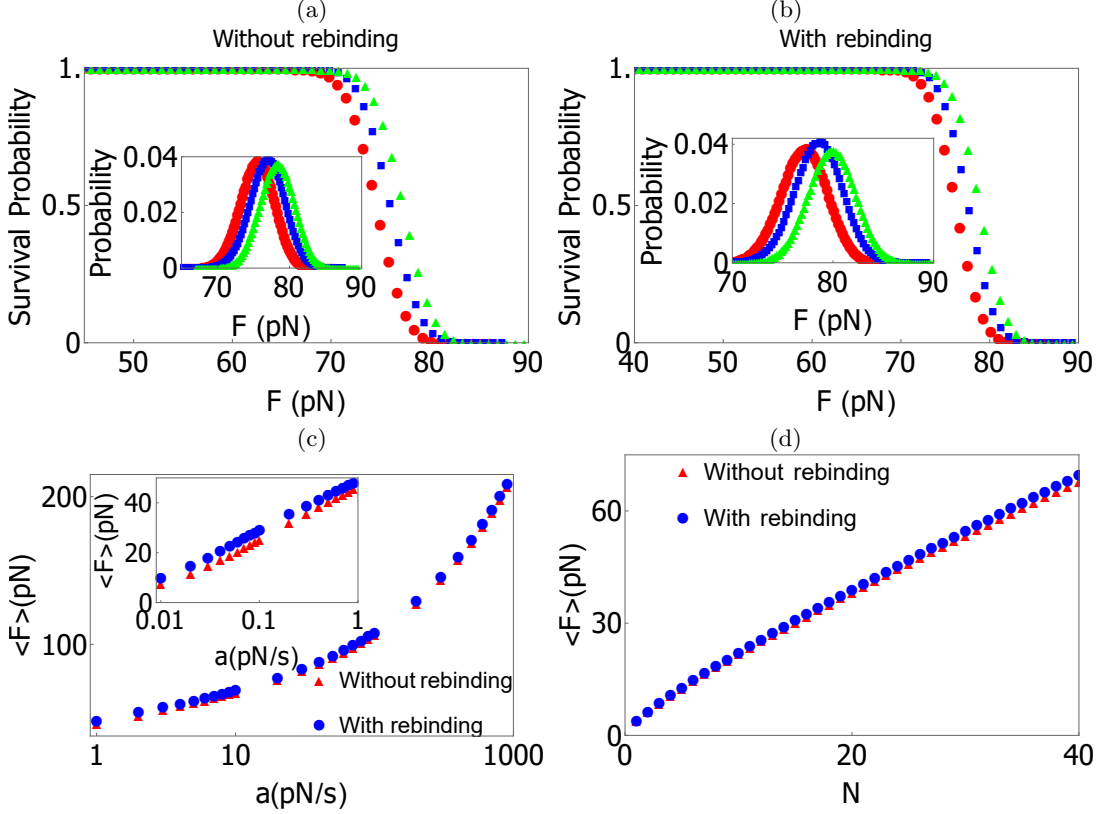


FIG. 6. Survival probabilities for three different loading rates $a = 18$ pN/s (red circle), 20 pN/s (blue square) and 22 pN/s (green triangle) are plotted (a) in the absence of rebinding and (b) in the presence of rebinding. In the inset the corresponding distributions of the rupture forces are shown. Mean rupture force is plotted against (c) the loading rate a for a fixed $N = 40$, and (d) N for a fixed loading rate $a = 10$ pN/s. Logarithmic scale is used along the X-axis in (c) to cover a very broad range of a . In the inset of (c) the mean rupture force is plotted for lower loading rate where the difference between the results for the two cases (without and with rebinding) is significant. The numerical values of all the other parameters are listed in the table I.

V. SUMMARY AND CONCLUSION

In this paper we have developed theoretical models to study the strength and stability of molecular joints formed by $N (\geq 1)$ parallel MT filaments with a single kt. We draw analogies between the kt-MT attachments and the common chemical ligand-receptor bonds where the kt is the analog of the receptor while each MT plays the role of a ligand. We also stress that, in spite of these superficial similarities, there are several crucial differences. The main sources of these differences arise from the fact that (i) each MT tip can grow or shrink because of ongoing polymerization or depolymerization of the MT and (ii) the rate of depolymerization is strongly suppressed by externally applied tension.

The strength and stability of non-covalent ligand-receptor bonds are routinely probed by dynamic force spectroscopy [19]. The rupture of such weak bonds is a thermally activated process; the external force alters the potential landscape thereby affecting its strength and stability, i.e., assist or oppose the thermally activated rupture process. Because of the intrinsic stochasticity of the rupture process, the lifetime and the rupture force are randomly distributed quantities. Therefore, repetition of the force-clamp and force-ramp experiments yield the probability densities of the lifetimes and rupture forces, respectively. Rupture dynamics of single ligand-receptor bonds as well as that of multiple ligand-receptor bonds in parallel have been studied both theoretically and experimentally for decades [30–35]. In the same spirit, we model and analyze the kt-MT attachment as an unusual ligand-receptor bond.

In this paper we have briefly reviewed the SSC model of rupture of attachments, consisting initially of a single kt and a single MT in force-clamp set up. Experimental data corresponding to the force-clamp set up have been reported [13]. Theories at different levels of molecular detail have been developed in the last few years to account for some unusual trends of variation observed with varying force in those experimental data [13, 18, 44]. In this paper we have

extended the SSC model to the more general case where the attachment initially consists of $N(> 1)$ MTs attached simultaneously to a single kt. Moreover, the model is formulated in such a way that it can be appropriately adapted to study the effects of either clamp force or ramp force. The results of our theoretical investigation reported here display complementary signatures of the catch-bond-like behavior of the single kt - single MT attachments subjected to ramp force. The evidences in favor of catch-bond-like behavior are also obtained from our numerical studies of the model in the more general case where initially $N(> 1)$ MTs are attached to a single kt. Both the mean lifetime and mean rupture force are found to scale nonlinearly with N .

In the force-clamp set up with optical trap, the bead-trap separation is maintained at a fixed value with a computer controlled feedback while the change in the length of the MT is recorded by monitoring the movement of the specimen stage [10]. A force-ramp set up, where the bead-trap separation is gradually increased with time, has also been designed by modifying the force-clamp software [10]. This force-ramp can be used to test the corresponding theoretical predictions made in this paper. To our knowledge, no experimental data are available at present to make direct comparison with the predictions of the general model developed here. However, very recent experimental breakthroughs [12] suggest that both force-clamp and force-ramp experiments with reconstituted mammalian kinetochores *in-vitro* may become possible in near future.

Acknowledgements:

One of the authors (DC) thanks Charles Asbury for valuable comments on a shorter preliminary draft of this manuscript. DC also thanks Raymond Friddle and Gaurav Arya for useful correspondences. This work has been supported by a J.C. Bose National Fellowship (DC) and “Prof. S. Sampath Chair” Professorship (DC).

-
- [1] T. Wittmann, A. Hyman and A. Desai, Nat. Cell Biol. **3**, E28 (2001).
 - [2] E. Karsenti and I. Vernos, Science **294**, 543 (2001).
 - [3] K.J. Helmke, R. Heald and J.D. Wilbur, Int. Rev. Cell Mol. Biol. **306**, 83 (2013).
 - [4] J.R. McIntosh, M.I. Molodtsov and F.I. Ataullakhanov, Quart. Rev. Biophys. (2012).
 - [5] J. L.D. Lawson and R.E. C. Salas, Biochem. Soc. Trans. **41**, 1736 (2013).
 - [6] A. Desai and T.J. Mitchison, Annu. Rev. Cell Dev. Biol. **13**, 83 (1997).
 - [7] I.M. Cheeseman, Cold Spring Harb. Perspect. Biol. 6:a015826 (2014).
 - [8] S. Biggins, genetics **194**, 817 (2013).
 - [9] B. Akiyoshi and S. Biggins, Chromosoma **121**, 235 (2012).
 - [10] A.D. Franck, A.F. Powers, D.R. Gestaut, T.N. Davis and C.L. Asbury, Methods **51**, 242 (2010).
 - [11] K.K. Sarangapani and C.L. Asbury, Trends in Genet. **30**, 150 (2014).
 - [12] J.R. Weir et al. Nature **537**, 249 (2016).
 - [13] B. Akiyoshi, K. K. Sarangapani, A. F. Powers, C. R. Nelson, S. L. Reichow, H. Arellano-Santoyo, T. Gonen, J. A. Ranish, C. L. Asbury and S. Biggins, Nature **468**, 576 (2010).
 - [14] W. E. Thomas, Annu. Rev. Biomed. Eng. **10**, 39 (2008).
 - [15] W. E. Thomas, V. Vogel and E. Sokurenko, Annu. Rev. Biophys. **37**, 399 (2008).
 - [16] E.V. Sokurenko, V. Vogel and W.E. Thomas, Cell Host & Microbe **4**, 314 (2008).
 - [17] O.V. Prezhdo and Y.V. Pereverzev, Acc. Chem. Res. **42**, 693 (2009).
 - [18] A. K. Sharma, B. Shtylla and D. Chowdhury, Phys. Biol. **11**, 1478 (2014).
 - [19] A.R. Bizzarri and S. Cannistraro (eds.) *Dynamic Force Spectroscopy and Biomolecular Recognition*, (CRC Press, 2012).
 - [20] T. Hill, Proc. Natl. Acad. Sci. U.S.A. **82**, 4404 (1985).
 - [21] G.J. Buttrick and J.B.A. Millar, Chromosome Res. **19**, 393 (2011).
 - [22] S. Westermann, D.G. Drubin and G. Barnes, Annu. Rev. Biochem. **76**, 563 (2007).
 - [23] T.N. Davis and L. Wordeman, Trends in Cell Biol. **17**, 377 (2007).
 - [24] E.A. Foley and T.M. Kapoor, Nat. Rev. Mo. Cell Biol. **14**, 25 (2013).
 - [25] A. D. Franck, A.F. Powers, D.R. Gestaut, T. Gonen, T. N. Davis and C.L. Asbury, Nat. Cell Biol. **9**, 832, (2007).
 - [26] H. Risken, *The Fokker-Planck Equation* (Springer, 1996).
 - [27] H. Wang, C. Peskin and T. Elston, J. Theo. Biol. **221**, 491 (2003).
 - [28] H. Wang, T. C. Elston, J. Stat. Phys. **128**, 35 (2007).
 - [29] G.I. Bell. Science, **200**, 618, (1978).
 - [30] E. Evans and K. Ritchie, Biophys. J., **72**, 1541, (1997).
 - [31] E. Evans, Annu. Rev. Biophys. Biomol. Struct. **30**, 105 (2001).
 - [32] E. Evan and P. Williams, in: *Phys. of Biomolecules and Cells*, eds. H. Flyvbjerg, F. Jülicher, F. Ormos and F. David (Springer and EDP Sciences, 2002).
 - [33] P. Williams, Anal. Chim. Acta., **479**, 107, (2003).
 - [34] R. W. Friddle, in: *Dynamic Force Spectroscopy and Biomolecular Recognition*, ed. A.R. Bizzarri and S. Cannistraro (CRC Press, 2012).
 - [35] G. Arya, Molec. Simul. **42**, 1102 (2016).
 - [36] A. P. Joglekar and A.J. Hunt, Biophys. J. **83**, 42 (2002).

- [37] B. Shtylla and J. P. Keener, SIAM J. Appl. Math. **71**, 1821 (2011).
- [38] S. Gonen, B. Akiyoshi, M.G. Iadanza, D. Shi, N. Duggan, S. Biggins, T. Gonen, Nat. Struct. Mol. Biol. **19**, 925 (2012).
- [39] A. P. Joglekar, D. Bouck, K. Finley, X. Liu, Y. Wan, J. Berman, X. He, E.D. Salmon and K.S. Bloom, J. Cell Biol. **181**, 587 (2008).
- [40] K. Johnston, A. Joglekar, T. Hori, A. Suzuki, T. Fukagawa, and E.D. Salmon, J. Cell Biol. **189**, 937 (2010).
- [41] A. P. Joglekar, D. C. Bouck, J. N. Molk, K. S. Bloom and E. D. Salmon, Nat. Cell Biol. **8**, 581 (2006).
- [42] J. C. Waters, T.J. Mitchison, C.L. Rieder and E. D. Salmon, Mol. Biol. Cell. **7**, 1547 (1996).
- [43] W. F. Marshall, J. F. Marko, D. A. Agard and J. W. Sedat, Curr. Biol. **11**, 569 (2001).
- [44] Z. Bertalan, C.A.M. La Porta, H. Maiato and S. Zapperi, Biophys. J. **107**, 289 (2014).
- [45] E. Evans, A. Leung, V. Heinrich and C. Zhu, PNAS **101**, 11281 (2004).
- [46] M. Dogterom and S. Leibler, Phys Rev Lett. **70**, 1347 (1993).